Received: *March 15, 2001*, Accepted: *March 27, 2001*
Revised: *March 26, 2001*

# String breaking from ladder diagrams in SYM theory

**Konstantin Zarembo**

*Department of Physics and Astronomy, and*
*Pacific Institute for the Mathematical Sciences*
*University of British Columbia*
*6224 Agricultural Road, Vancouver, B.C. Canada V6T 1Z1, and*
*Institute of Theoretical and Experimental Physics*
*B. Cheremushkinskaya 25, 117259 Moscow, Russia*
*E-mail:* zarembo@physics.ubc.ca

Abstract: The AdS/CFT correspondence establishes a string representation for Wilson loops in $\mathcal{N}=4$ SYM theory at large $N$ and large 't Hooft coupling. One of the clearest manifestations of the stringy behaviour in Wilson loop correlators is the string-breaking phase transition. It is shown that resummation of planar diagrams without internal vertices predicts the strong-coupling phase transtion in exactly the same setting in which it arises from the string representation.

Keywords: 1/N Expansion, AdS-CFT Correspondance.

JHEP03(2001)042

## Contents



## 1. Introduction

In its strongest form, the AdS/CFT correspondence establishes an equivalence of $\mathcal{N} = 4$ supersymmetric Yang-Mills (SYM) theory and string theory in Anti-de-Sitter space [1]–[4]. Because even a free string propagation in Anti-de-Sitter space is rather complicated, going beyond the low-energy, supergravity approximation in the AdS/CFT correspondence is extremely hard. Not surprisingly, the stringy nature of the AdS/CFT duality is not directly visible in the supergravity limit. Fortunately, there is one exception: Wilson loops in $\mathcal{N} = 4$ SYM probe genuine stringy degrees of freedom even in the supergravity regime [5, 6, 4, 7]. Wilson loop correlators therefore should display stringy behavior in the large-$N$, large 't Hooft coupling limit of SYM theory which is dual to classical supergravity.

One of the clearest manifestations of the stringy behavior in Wilson loop correlators is the string breaking phenomenon. A good example of the string breaking is Gross-Ooguri phase transition in the correlator of two Wilson loops [8]–[11]. When the loops are pulled apart, the string that connects them eventually breaks and the correlation function of the Wilson loops undergoes a phase transition. This phase transition looks rather unusual from the field theory perspective: each Feynman diagram that contributes to the Wilson loop correlator depends analytically on the distance between the loops. Of course, intuition based on individual Feynman graphs may well be wrong in the large 't Hooft coupling limit. To reach the strong coupling regime on the field theory side, one has to sum all planar diagrams, which is practically impossible in an interacting field theory such as $\mathcal{N} = 4$ SYM. It is thus rather surprising that partial resummation that takes into account only diagrams without internal vertices gives results remarkably similar to the supergravity predictions [12]–[16]. For a circular Wilson loop, diagrams without internal vertices reproduce all available predictions of string theory, including the area of classical string world-sheet [13] and the dimension of Teichmüller moduli space in string perturbation theory [14]. In fact, the sum of diagrams without internal vertices seems to give an exact result for the circular loop to all orders of $1/N^2$ expansion and for any 't Hooft coupling due to special conformal and supersymmetry transformation properties of the circular loop operator [14].

The diagrams without internal vertices definitely do not exhaust all possible contributions for other contours. For instance, the large-$N$ expectation value for a pair of anti-parallel Wilson lines receives contributions from all possible planar diagrams (though there are some unexpected cancellation in this case as well [13]). Nevertheless, the sum of ladder diagrams for anti-parallel lines extrapolated to the strong coupling limit qualitatively agrees with the predictions of AdS/CFT duality [12, 13]. In particular, the diagram resummation and the AdS/CFT correspondence predict the same degree of screening of electric charge at large 't Hooft coupling. Similar results were found in non-commutative $\mathcal{N}=4$ SYM theory [15].

These observations support the conjecture that resummation of diagrams without internal vertices always displays stringy behavior in the strong-coupling regime. To test this conjecture, I will sum up diagrams without internal vertices for a correlator of two Wilson loops to see if this resummation gives rise to the Gross-Ooguri phase transition.

The Gross-Ooguri phase transition in the correlator of Wilson loops is reviewed in section 2. In section 3, the same correlator is analyzed in the ladder diagram approximation.

## 2. Gross-Ooguri phase transition

The Wilson loop operator that has right transformation properties under supersymmetry [7] couples not only to gauge potentials, but also to the scalar fields, $\Phi_I$, $I=1,\ldots,6$, of $\mathcal{N}=4$ SYM theory [5, 6]:

$$P(C) = \mathrm{tr}\,\mathrm{P}\exp\left[\oint_C d\tau\ \left(iA_\mu(x)\dot{x}_\mu + \Phi_I(x)\theta_I|\dot{x}|\right)\right]. \tag{2.1}$$

Here, $\theta_I$ is a point on a five-dimensional unit sphere: $\theta^2=1$, and $x_\mu(\tau)$ parameterizes contour $C$. The coupling to scalars cancels potential UV divergences and Wilson loop correlators are finite for smooth contours [7, 13].

The AdS dual of this operator is a world-sheet of type IIB superstring that propagates in the bulk of AdS space and whose ends are attached to the contour $C$ on the boundary [5, 6]. The tension of the AdS string is dimensionless and, according to the AdS/CFT dictionary, is proportional to the square root of the 't Hooft coupling of SYM theory:

$$T = \frac{\sqrt{\lambda}}{2\pi}, \qquad \lambda = g_{\mathrm{YM}}^2 N.$$

The large-$N$, large 't Hooft coupling limit corresponds to a free string with very large tension, which suppresses all fluctuations of the string. Therefore, the string world-sheet is classical in the strong coupling limit, and Wilson loop correlators obey the minimal area law.

Actually, a straightforward implementation of the minimal area law does not work because of the divergence of the area due to a singular behavior of the AdS metric at the boundary. It was argued that the definition of the minimal area appropriate for computation of Wilson loop correlators involves the Legendre transform [7]. An alternative regularization is based on subtraction of the area of a reference surface with the same boundary [5]. In the semiclassical limit, these two regularizations are mathematically equivalent. It is not clear if this equivalence holds beyond the semiclassical limit, probably it does not, but at the semiclassical level, we are free to use either of the two regularizations. The regularization by subtraction then has an interesting consequence: since the subtracted area is always larger than the area of a minimal surface, regularized area is always *negative*. Hence,

$$\ln \langle P(C) \rangle = \sqrt{\lambda} \times (\text{positive number}) \tag{2.2}$$

at large $\lambda$. The AdS/CFT correspondence therefore predicts that Wilson loop expectation values exponentiate at strong coupling and that the exponent is proportional to $\sqrt{\lambda}$ with positive coefficient.

The minimal surface is unique only for simplest contours. In general, the area functional has several local minima, so the semiclassical string partition function receives contributions from several saddle points:

$$\langle P(C) \rangle = \sum \alpha_i \exp\left(-\frac{\sqrt{\lambda}\, A_i}{2\pi}\right), \tag{2.3}$$

where $A_i$ are (negative) regularized areas of locally minimal surfaces and $\alpha_i = \lambda^{-3/4} \times (\text{power series in } 1/\sqrt{\lambda})$ represent quantum corrections due to fluctuations of the string world sheet [14],[17]–[21]. At large $\lambda$, the term with the smallest area dominates. Of course, each $A_i$ smoothly depends on geometric parameters of the contour $C$, so the Wilson loop expectation value is a smooth function of $C$, but its large-$\lambda$ asymptotics, in general, is not, because different terms in the sum (2.3) may dominate for contours of different shapes. If the shape of a contour is continuously changed, two local minima can become degenerate and the semiclassical partition function will switch from one saddle point to another. The large-$\lambda$ asymptotics of the Wilson loop will then undergo a phase transition. This phenomenon is generic for semiclassical amplitudes and was encountered for instance, in the study of sphaleron transitions in quantum mechanics [22] or in quantum field theory [23]–[25]. In the context of string representation for Wilson loops, the existence of a phase transition due to rearrangement of minimal surfaces was pointed out by Gross and Ooguri [8], and has been studied in much detail in [9, 10].



JHEP03(2001)042

The simplest correlation function that undergoes the string-breaking phase transition is the connected correlator of two Wilson loops:

$$W(C_1, C_2) = \langle P(C_1)P(C_2)\rangle - \langle P(C_1)\rangle \langle P(C_2)\rangle \ , \tag{2.4}$$

where $C_1$ and $C_2$ are identical circles of opposite orientation separated by distance $L$. At strong coupling, the correlator is dominated by the string world-sheet stretched between the two contours (figure 1). When the contours are pulled apart, the string will eventually break, and the disconnected surface with the topology of two disks (figure 2) will become a global minimum. The connectedness of the correlator is then achieved by perturbative exchange of supergravity modes between separate minimal surfaces [8, 26].

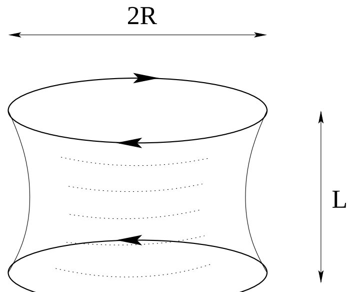


**Figure 1:** Connected minimal surface.

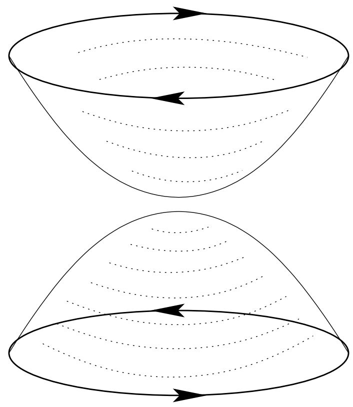

**Figure 2:** Disconnected minimal surface.

The above intuitive arguments do not take into account the strong curvature of $AdS_5 \times S^5$ background in which the strings propagate. However, an explicit solution for semiclassical string world-sheet [9]–[11] shows that the curvature of AdS space does not alter the qualitative picture of the Gross-Ooguri phase transition. In figure 3, the logarithm of the two-loop correlator (proportional to minus an area of the minimal surface) computed in [9, 10] is plotted as a function of the distance between the loops.

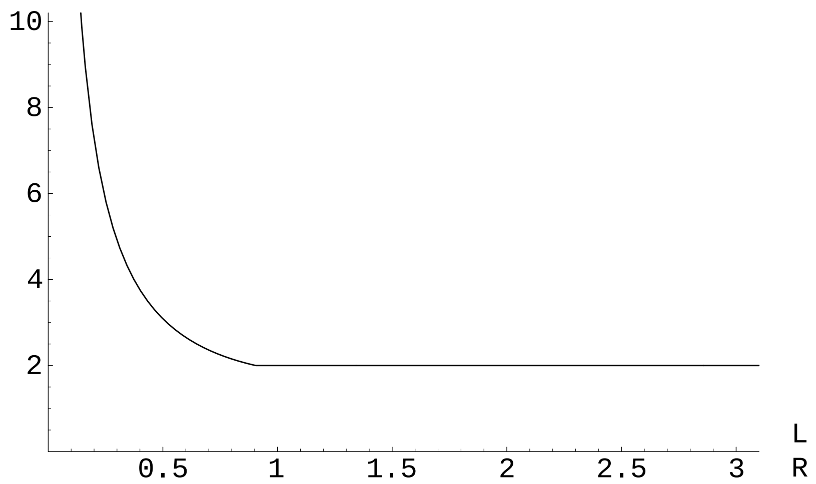


**Figure 3:** $\ln W(C_1, C_2)/\sqrt{\lambda}$ as a function of the distance between the loops.

It is important to note that if the circles had the same orientation, the connected minimal surface would not have existed. Consequently, the phase transition takes place only for anti-parallel circles and there is no phase transition when the circles are parallel.

## 3. Ladder diagrams

In this section, I will calculate the contribution of all planar Feynman diagrams without internal vertices to the correlator of two circular Wilson loops. This amounts in replacement of the vacuum expectation value in (2.4) by an average over free fields. In the Feynman gauge, the Wick contraction of the exponent in the Wilson loop operator is

$$\left\langle \left(iA_\mu(x)\dot{x}_\mu + \Phi_I(x)\theta_I|\dot{x}|\right)_{ij} \left(iA_\mu(y)\dot{y}_\mu + \Phi_I(y)\theta_I|\dot{y}|\right)_{kl} \right\rangle_0 = \frac{1}{N}\,\delta_{il}\delta_{jk}\,\lambda\,\frac{|\dot{x}||\dot{y}| - \dot{x}\cdot\dot{y}}{8\pi^2|x-y|^2}\,, \tag{3.1}$$

where $i, j, k, l$ are U($N$) group indices.

It is important to note that separation of all planar graphs in the diagrams with and without internal vertices is not gauge invariant and is consistent only in the Feynman gauge, because only in the Feynman gauge these classes of diagrams are separately UV finite. Any other gauge condition brings in spurious divergences which invalidate resummation of diagrams without internal vertices. The finiteness in the Feynman gauge is a consequence of SO(10) symmetry that rotates vector and scalar fields of $\mathcal{N} = 4$ SYM and is inherited from ten-dimensional Lorentz invariance. This symmetry is broken by any other gauge condition, as well as by interaction terms.

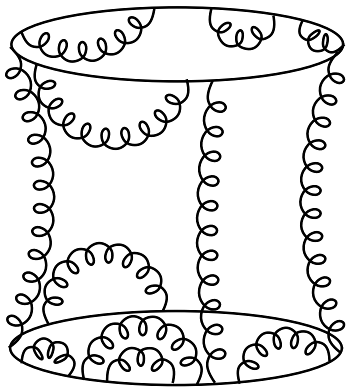

**Figure 4:** A typical diagram that contributes to the connected correlator of Wilson loops in the free-field approximation.

A typical planar diagram without internal vertices that contributes to the connected correlator of two Wilson loops (figure 4) consists of rainbow propagators, which are attached to one of the loops, and ladder propagators, which connect the two loops together. In spirit of the usual identification of planar diagrams with discretized random surfaces [27], it is natural to associate ladder diagrams with connected string world-sheets (figure 1) and rainbow graphs with the disconnected surfaces (figure 2). If the distance between the circles is large compared to their radii, ladder diagrams are suppressed. The large-$\lambda$ asymptotics is then governed by exponentiation of rainbow graphs. The known sum of rainbow diagrams [13] dictates the following asymptotic behavior of the correlator at large separation between the



JHEP03(2001)042

contours:

$$W(C_1, C_2) \sim \langle P(C_1) \rangle \langle P(C_2) \rangle \approx \mathrm{e}^{\,2\sqrt{\lambda}} \qquad (L \gg R)\,. \tag{3.2}$$

This exactly coincides with the AdS/CFT prediction [26, 7], figure 3. In particular, the exponent in (3.2) does not depend on $L$ or $R$.

In the opposite limit of very small $L$ or of very large $R$, the circles can be approximated by anti-parallel lines. In that case, ladder diagrams evidently dominate. The large-$\lambda$ extrapolation of their sum is also known [12, 13] and implies the following asymptotics of the Wilson loop correlator at small separation between the loops:

$$W(C_1, C_2) \sim \mathrm{e}^{\,2\sqrt{\lambda}R/L} \qquad (L \ll R)\,. \tag{3.3}$$

The scaling with $\lambda$, $R$ and $L$ is again correct, but the numerical coefficient in the exponent somewhat exceeds the AdS/CFT prediction.

An exact resummation of ladder and rainbow diagrams shows that asymptotics (3.2) and (3.3) do not match smoothly. There is a phase transition at $L_c = 2R$, at which the correlator ceases to depend on the distance and the asymptotics (3.2) sets on. This phase transition can be associated with breaking of the string made of ladder diagrams. In the large-distance phase, the large-$\lambda$ behavior of the correlator is entirely determined by rainbow graphs, while in the short-distance phase, rainbow and ladder graphs are equally important.

It is convenient to split the calculation into two parts: first resum rainbow graphs, and then write down Dyson equation for ladder diagrams. Let us denote the sum of the rainbow graphs for an arc between polar angles $\theta$ and $\theta'$ by $W(\theta' - \theta)$:

$W(\theta' - \theta) =$ 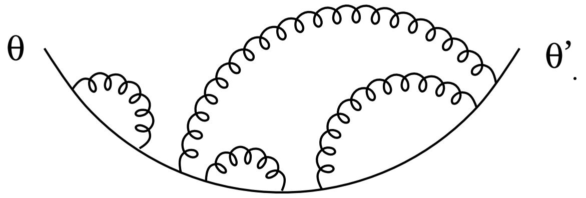

. (3.4)

Each rainbow propagator in this sum is a constant, because, for a circular contour,

$$\frac{|\dot{x}(\theta_1)||\dot{x}(\theta_2)| - \dot{x}(\theta_1)\cdot\dot{x}(\theta_2)}{|x(\theta_1) - x(\theta_2)|^2} = \frac{1}{2} \tag{3.5}$$

independently of $\theta_1$ and $\theta_2$. The summation of the rainbow graphs then reduces to a zero-dimensional problem:

$$W(s) = \left\langle \mathrm{e}^{\,sM} \right\rangle\,, \tag{3.6}$$

where gaussian average over hermitean $N \times N$ matrix $M$ is defined to reproduce the SYM Wick contraction (3.1):

$$\langle F(M) \rangle = \frac{1}{Z}\int dM\, F(M) \exp\left(-\frac{8\pi^2}{\lambda} N \operatorname{tr} M^2\right)\,. \tag{3.7}$$



JHEP03(2001)042

The average (3.6) can be calculated using standard techniques of large-$N$ random matrix models [28]–[30]. In fact, it is easier to find the Laplace transform of $W(s)$:

$$W(z) \equiv \int_0^\infty ds\, \mathrm{e}^{-zs} W(s) = \left\langle \frac{1}{z-M} \right\rangle = \frac{8\pi^2}{\lambda}\left(z - \sqrt{z^2 - \frac{\lambda}{4\pi^2}}\right). \tag{3.8}$$

The inverse Laplace transform yields:

$$W(s) = \frac{2}{\sqrt{\lambda s}}\, I_1\left(\sqrt{\lambda s}\right), \tag{3.9}$$

where $I_1$ is the modified Bessel function.

For a ladder propagator that connects two loops,

$$\frac{|\dot{x}_1(\theta_1)||\dot{x}_2(\theta_2)| - \dot{x}_1(\theta_1)\cdot\dot{x}_2(\theta_2)}{|x_1(\theta_1) - x_2(\theta_2)|^2} = \frac{1}{2}\,\frac{1+\cos(\theta_1-\theta_2)}{\frac{L^2}{2R^2} + 1 - \cos(\theta_1-\theta_2)} \equiv G(\theta_1-\theta_2), \tag{3.10}$$

where $x_1(\theta)$, $x_2(\theta)$ parameterize the separate circles. The connected correlator of Wilson loops contains at least one such propagator, which we extract from the sum, for later convenience:

$$W(C_1, C_2) = \frac{\lambda}{4\pi}\int_0^{2\pi} d\varphi\, G(\varphi)\Gamma(2\pi, 2\pi; \varphi). \tag{3.11}$$

All of the rest contributions can be found by solving Dyson equation:

$$\Gamma(s,t;\varphi) = W(s)W(t) + \frac{\lambda}{8\pi^2}\int_0^s ds' \int_0^t dt'\, W(s-s')W(t-t')G(s'-t'+\varphi)\Gamma(s',t';\varphi), \tag{3.12}$$

supplemented by boundary conditions:

$$\Gamma(0,t;\varphi) = \Gamma(s,0;\varphi) = 0. \tag{3.13}$$

Iteration of this equation reproduces the sum of ladder diagrams with all possible insertions of rainbow propagators.

Again, it is useful to do the Laplace transform:

$$\Gamma(z,w;\varphi) = \int_0^\infty ds \int_0^\infty dt\, \mathrm{e}^{-zs-wt}\,\Gamma(s,t;\varphi), \tag{3.14}$$

after which the Dyson equation takes the form:

$$\Gamma(z,w;\varphi) = W(z)W(w)\left(1 + \frac{\lambda}{8\pi^2}\sum_n \mathrm{e}^{in\varphi} G_n \Gamma(z-in, w+in; \varphi)\right), \tag{3.15}$$

where $G_n$ are Fourier modes of $G(\theta)$:

$$G(\theta) = \sum_n G_n\, \mathrm{e}^{in\theta}. \tag{3.16}$$



JHEP03(2001)042

Singularities of the kernel $\Gamma(z, w; \varphi)$ at complex $z$ and $w$ essentially determine its inverse Laplace transform. To get an idea of the range of $z$ and $w$ in which the singularities occur, let us consider an iterative solution of the Dyson equation (3.15). To the first approximation, the kernel factorizes on two separate sums of rainbow diagrams: $\Gamma(z, w; \varphi) = W(z)W(w)$. The singularities are branch cuts across the real axes in the complex $z$ and $w$ planes with branch points at $\pm\sqrt{\lambda}/2\pi$. A first iteration of eq. (3.15) will shift cuts into the complex plane and branch points at $\pm\sqrt{\lambda}/2\pi + in$ will arise for any integer $n$. Next iterations do not produce any new singularities. In the most interesting regime of large $\lambda$, the branch cuts extend to large distances of order of $\sqrt{\lambda}$ along the real axis. It is therefore convenient to rescale $z$ and $w$ by $\sqrt{\lambda}/2\pi$. The form of eq. (3.15) then suggests the following change of variables:

$$\Gamma\left(\frac{\sqrt{\lambda}}{2\pi}(\omega + ip), \frac{\sqrt{\lambda}}{2\pi}(\omega - ip); \varphi\right) = \frac{4\pi^2}{\lambda}\, \mathrm{e}^{\frac{i\sqrt{\lambda}p\varphi}{2\pi}} L(\omega, p)\,. \tag{3.17}$$

The dependence on $\varphi$ trivially follows from the Dyson equation (3.15). Introducing the notation:

$$D(\omega) \equiv \frac{2\pi}{\sqrt{\lambda}} \frac{1}{W\left(\frac{\sqrt{\lambda}}{2\pi}\omega\right)} = \frac{1}{2}\left(\omega + \sqrt{\omega^2 - 1}\right), \tag{3.18}$$

we can rewrite the Dyson equation as

$$D(\omega + ip)D(\omega - ip)L(\omega, p) - \frac{1}{2}\sum_n G_n L\left(\omega, p - \frac{2\pi n}{\sqrt{\lambda}}\right) = 1\,. \tag{3.19}$$

The Fourier transform in $p$,

$$L(\omega, x) = \frac{\sqrt{\lambda}}{4\pi^2}\int_{-\infty}^{+\infty} dp\; \mathrm{e}^{\frac{i\sqrt{\lambda}px}{2\pi}} L(\omega, p)\,, \tag{3.20}$$

then yields a Schrödinger-like equation:

$$\left[D\left(\omega + \frac{2\pi}{\sqrt{\lambda}}\frac{d}{dx}\right) D\left(\omega - \frac{2\pi}{\sqrt{\lambda}}\frac{d}{dx}\right) - \frac{1}{2}G(x)\right] L(\omega, x) = \delta(x) \tag{3.21}$$

with the hamiltonian

$$H(p, x; \omega) = D(\omega + ip)D(\omega - ip) - \frac{1}{2}G(x)\,, \tag{3.22}$$

where the momentum operator is defined as

$$p = -i\,\frac{2\pi}{\sqrt{\lambda}}\frac{d}{dx}\,. \tag{3.23}$$

The formal solution of the Schrödinger equation (3.21) is

$$L(\omega, x) = \left\langle x \middle| H^{-1}(\omega) \middle| 0 \right\rangle\,. \tag{3.24}$$

Here $|0\rangle$ is the zero eigenstate of the coordinate operator:

$$x|0\rangle = 0\,. \tag{3.25}$$

In terms of the complete set of eigenfunctions of $H$:[1]

$$L(\omega, x) = \sum_n \frac{\psi_n^*(0;\omega)\psi_n(x;\omega)}{E_n(\omega)}\,. \tag{3.26}$$

The wave functions $\psi_n$ satisfy the Schrödinger equation

$$H\left(-i\frac{2\pi}{\sqrt{\lambda}}\frac{d}{dx}, x; \omega\right)\psi_n(x;\omega) = E_n(\omega)\psi_n(x;\omega)\,, \tag{3.27}$$

and are properly normalized.

The kernel $\Gamma$ with coinciding arguments determines the expectation value of the Wilson loop correlator, according to (3.11). Its Laplace transform can be easily found with the help of (3.17), (3.20):

$$\begin{aligned}\int_0^\infty ds\,\mathrm{e}^{-\frac{\sqrt{\lambda}\omega s}{\pi}}\Gamma(s,s;\varphi) &= \frac{\sqrt{\lambda}}{4\pi^2}\int_{-\infty}^{+\infty} dp\,\Gamma\left(\frac{\sqrt{\lambda}}{2\pi}(\omega - ip), \frac{\sqrt{\lambda}}{2\pi}(\omega + ip); \varphi\right)\\ &= \frac{4\pi^2}{\lambda}\,L(\omega,\varphi)\,.\end{aligned} \tag{3.28}$$

The inverse Laplace transform gives:

$$\Gamma(s,s;\varphi) = \frac{2}{i\sqrt{\lambda}}\int_{C-i\infty}^{C+i\infty} d\omega\,\mathrm{e}^{\frac{\sqrt{\lambda}\omega s}{\pi}}L(\omega;\varphi)\,, \tag{3.29}$$

where the contour of integration passes all singularities of the integrand from the right. Substitution of the solution of the Schrödinger equation (3.26) into (3.29) gives for the Wilson loop expectation value:

$$W(C_1,C_2) = \frac{\sqrt{\lambda}}{2\pi i}\int_{C-i\infty}^{C+i\infty} d\omega\,\mathrm{e}^{2\sqrt{\lambda}\omega}\sum_n \frac{1}{E_n(\omega)}\,\psi_n^*(0;\omega)\int_0^{2\pi} d\varphi\,G(\varphi)\psi_n(\varphi;\omega)\,. \tag{3.30}$$

This expression is valid for any $\lambda$ and, in particular, for large $\lambda$. It actually simplifies in the strong-coupling limit, because then the integrand in (3.30) rapidly oscillates and the integral over $\omega$ is saturated by the singularity of the integrand in the complex $\omega$ plane with the largest real part:[2]

$$W(C_1,C_2) \simeq \mathrm{e}^{2\sqrt{\lambda}\omega_0}\,. \tag{3.31}$$

[1]Since the potential $G(x)$ is periodic, the spectrum of $H$ will form a band structure, so, strictly speaking, summation over eigenvalues should be understood as an integration weighted with the density of states

[2]It can be shown that such a singularity lies on the positive real semi-axis.



JHEP03(2001)042

Therefore, diagrams without internal vertices exponentiate, and the exponent is proportional to $\sqrt{\lambda}$ with positive coefficient, in agreement with general properties of the AdS/CFT prediction.

It is not hard to find $\omega_0$ in the limit of large $\lambda$. There are two sources of non-analyticity in the integrand of (3.30): (i) when $E_n(\omega)$ hits zero, the integrand develops a pole[3] and (ii) each $E_n(\omega)$ is a multivalued function because the hamiltonian (3.22) is not analytic in $\omega$.

The reason for simplification at large $\lambda$ stems from the commutation relation

$$[x,p]=i\frac{2\pi}{\sqrt{\lambda}}\,, \tag{3.32}$$

which shows that $2\pi/\sqrt{\lambda}$ plays the role of the Plank constant. The large-$\lambda$ limit is therefore semiclassical. The semiclassical spectrum of the hamiltonian (3.22), which is self-adjoined at real $\omega$, forms a continuum that starts from the minimum of the classical energy in the phase space:

$$\lim_{\lambda\to\infty} E_0(\omega)=\min_{p,x} H(p,x;\omega)\,. \tag{3.33}$$

The kinetic energy is minimal at zero momentum. The minimum of the potential is reached at $x=0$, so

$$E_0(\omega)\approx\Big(D(\omega)\Big)^2-\frac{1}{2}\,G(0)=\frac{1}{4}\,\Big(\omega+\sqrt{\omega^2-1}\Big)^2-\frac{R^2}{L^2}\,. \tag{3.34}$$

The ground state energy always has a branch point at $\omega_0=1$. This singularity originates from the square root branch point in the sum of rainbow graphs (3.8) at $z=\sqrt{\lambda}/2\pi$ and translates into the distance-independent large-$\lambda$ asymptotics (3.2) for the Wilson loop correlator. Another singularity arises when $E_0$ crosses zero. This happens at

$$\omega_0=\frac{R}{L}+\frac{L}{4R},$$

provided that $L<2R$, otherwise eigenvalues of the hamiltonian (3.22) are positive for any $\omega>1$. At distances larger than $L_c=2R$, the branch point at $\omega=1$ is the only singularity of the integrand in (3.30). At smaller distances, the integrand has a pole at larger $\omega$ in addition to the branch cut. Thus

$$\omega_0=\begin{cases}1, & L>2R\\ \dfrac{R}{L}+\dfrac{L}{4R}\,, & L<2R\end{cases}\,, \tag{3.35}$$

and, consequently,

$$W(C_1,C_2)\simeq\begin{cases}\mathrm{e}^{\,2\sqrt{\lambda}}, & L>2R\\ \mathrm{e}^{\,\sqrt{\lambda}\left(\frac{2R}{L}+\frac{L}{2R}\right)}, & L<2R\end{cases}\,. \tag{3.36}$$

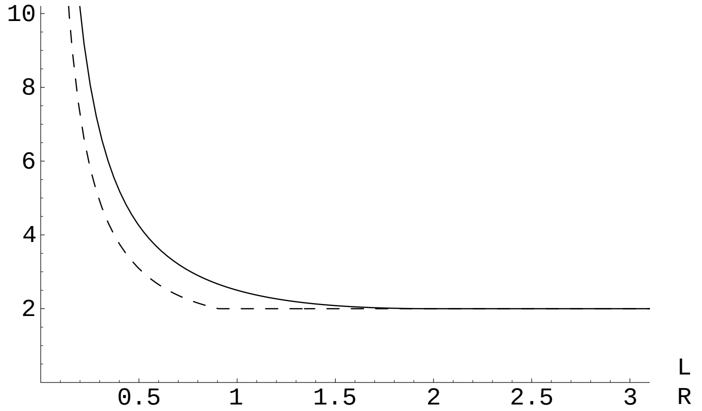


**Figure 5:** $\ln W(C_1, C_2)/\sqrt{\lambda}$ as a function of the distance between the loops. The solid curve represents the result of resummation of diagrams without internal vertices extrapolated to the strong coupling. The dashed curve is the AdS/CFT prediction.



Thus, the Wilson loop expectation value undergoes a phase transition at large $\lambda$ in the ladder diagram approximation. This phase transition is completely analogous to the Gross-Ooguri transition in the semiclassical string amplitude. At large distances, the expectation value is dominated by rainbow diagrams that can be associated with disconnected string world-sheets. The field theory calculation agrees exactly with the prediction of AdS/CFT correspondence in this case for the reasons explained in [14]. At short distances, ladder graphs, which are counterparts of the connected world-sheets, become increasingly important. Despite the lack of apparent reasons for the field theory calculation to be accurate in the short-distance phase, the result of the diagram resummation only slightly deviates from the AdS/CFT prediction (figure 5).

It is straightforward to repeat resummation of the diagrams without internal vertices for parallel circles. The inversion of the orientation changes sign in the numerator of (3.10):

$$\tilde{G}(\theta_1-\theta_2) \equiv \frac{|\dot{x}_1(\theta_1)||\dot{x}_2(\theta_2)| - \dot{x}_1(\theta_1)\cdot\dot{x}_2(\theta_2)}{|x_1(\theta_1)-x_2(\theta_2)|^2} = \frac{1}{2}\,\frac{1-\cos(\theta_1-\theta_2)}{\frac{L^2}{2R^2}+1-\cos(\theta_1-\theta_2)}\,. \tag{3.37}$$

All subsequent calculations remain the same up to replacement of $G$ by $\tilde{G}$. In particular, (3.30) still holds, but the large-$\lambda$ limit of the ground state energy now is given by

$$\tilde{E}_0(\omega) \approx \Big(D(\omega)\Big)^2 - \frac{1}{2}\,\tilde{G}(\pi) = \frac{1}{4}\,\Big(\omega+\sqrt{\omega^2-1}\Big)^2 - \frac{R^2}{L^2+2R^2}\,, \tag{3.38}$$

because the potential, $-\tilde{G}(x)$, has a minimum at $x=\pi$. This expression turns out to be positive for any $R$ and $L$, which means that energy levels never cross zero, so

[3]To be more precise, the energy spectrum is continuous, so the poles associated with distinct energy levels fuse and form a cut.

the only source of non-analyticity in $\omega$ is the branch point associated with rainbow diagrams. Consequently, there is no string-breaking phase transition, in agreement with what is expected from AdS/CFT correspondence. In fact, the string theory prediction for parallel circles is reproduced exactly, since rainbow graphs always dominate:

$$W(C_1, \tilde{C}_2) \approx \mathrm{e}^{\,2\sqrt{\lambda}}\,. \tag{3.39}$$

## 4. Discussion

Retaining only Feynman graphs without internal vertices is well motivated at strong coupling only in a special case of the circular Wilson loop. However, resummation of such diagrams bears a qualitative agreement with AdS/CFT correspondence for all Wilson loop correlators studied so far. The strong coupling asymptotics of the resummed perturbative series is always of the form (2.2), which is a general prediction of the string theory. In the case of the two-loop correlator, the resummed ladder diagrams undergo a strong-coupling phase transition when we expect the string breaking to occur and depend analytically on the distance between the loops when string breaking does not happen. Results of perturbative calculation do not deviate much from the AdS/CFT prediction even quantitatively, which allows us to speculate that resummation of diagrams without internal vertices may in general constitute a first approximation of some systematic expansion, and that there may be a more direct link between planar diagrams without internal vertices and strings.

## Acknowledgments

I am grateful to G. Semenoff and C. Thorn for discussions. This work was supported by NSERC of Canada, by Pacific Institute for the Mathematical Sciences and in part by RFBR grant 98-01-00327 and RFBR grant 00-15-96557 for the promotion of scientific schools.

## References

[1] J. Maldacena, *The large-N limit of superconformal field theories and supergravity*, *Adv. Theor. Math. Phys.* **2** (1998) 231 [`hep-th/9711200`].

[2] S.S. Gubser, I.R. Klebanov and A.M. Polyakov, *Gauge theory correlators from non-critical string theory*, *Phys. Lett.* **B 428** (1998) 105 [`hep-th/9802109`].

[3] E. Witten, *Anti-de Sitter space and holography*, *Adv. Theor. Math. Phys.* **2** (1998) 253 [`hep-th/9802150`].

[4] O. Aharony, S.S. Gubser, J. Maldacena, H. Ooguri and Y. Oz, *Large-N field theories, string theory and gravity*, *Phys. Rep.* **323** (2000) 183 [`hep-th/9905111`].

[5] J. Maldacena, *Wilson loops in large-N field theories*, *Phys. Rev. Lett.* **80** (1998) 4859 [hep-th/9803002].

[6] S.-J. Rey and J. Yee, *Macroscopic strings as heavy quarks in large-N gauge theory and anti-de Sitter supergravity*, hep-th/9803001.

[7] N. Drukker, D.J. Gross and H. Ooguri, *Wilson loops and minimal surfaces*, *Phys. Rev.* **D 60** (1999) 125006 [hep-th/9904191].

[8] D.J. Gross and H. Ooguri, *Aspects of large-N gauge theory dynamics as seen by string theory*, *Phys. Rev.* **D 58** (1998) 106002 [hep-th/9805129].

[9] K. Zarembo, *Wilson loop correlator in the AdS/CFT correspondence*, *Phys. Lett.* **B 459** (1999) 527 [hep-th/9904149].

[10] P. Olesen and K. Zarembo, *Phase transition in Wilson loop correlator from AdS/CFT correspondence*, hep-th/0009210.

[11] H. Kim, D.K. Park, S. Tamarian and H.J. W. Muller-Kirsten, *Gross-Ooguri phase transition at zero and finite temperature: two circular Wilson loop case*, *J. High Energy Phys.* **03** (2001) 003 [hep-th/0101235].

[12] J.K. Erickson, G.W. Semenoff, R.J. Szabo and K. Zarembo, *Static potential in $N = 4$ supersymmetric Yang-Mills theory*, *Phys. Rev.* **D 61** (2000) 105006 [hep-th/9911088].

[13] J.K. Erickson, G.W. Semenoff and K. Zarembo, *Wilson loops in $N = 4$ supersymmetric Yang-Mills theory*, *Nucl. Phys.* **B 582** (2000) 155 [hep-th/0003055].

[14] N. Drukker and D.J. Gross, *An exact prediction of $N = 4$ susym theory for string theory*, hep-th/0010274.

[15] M. Rozali and M.V. Raamsdonk, *Gauge invariant correlators in non-commutative gauge theory*, hep-th/0012065.

[16] G. Akemann and P.H. Damgaard, *Wilson loops in $N = 4$ supersymmetric Yang-Mills theory from random matrix theory*, hep-th/0101225.

[17] N. Drukker, D.J. Gross and A. Tseytlin, *Green-Schwarz string in $AdS_5 \times S^5$: semi-classical partition function*, *J. High Energy Phys.* **04** (2000) 021 [hep-th/0001204].

[18] S. Förste, D. Ghoshal and S. Theisen, *Stringy corrections to the Wilson loop in $N = 4$ super Yang-Mills theory*, *J. High Energy Phys.* **08** (1999) 013 [hep-th/9903042].

[19] J. Greensite and P. Olesen, *Remarks on the heavy quark potential in the supergravity approach*, *J. High Energy Phys.* **08** (1998) 009 [hep-th/9806235].

[20] S. Naik, *Improved heavy quark potential at finite temperature from anti-de Sitter supergravity*, *Phys. Lett.* **B 464** (1999) 73 [hep-th/9904147].

[21] Y. Kinar, E. Schreiber, J. Sonnenschein and N. Weiss, *Quantum fluctuations of Wilson loops from string models*, *Nucl. Phys.* **B 583** (2000) 76 [hep-th/9911123].

[22] E.M. Chudnovsky, *Phys. Rev.* **A 46** (1992) 8011.

[23] S. Habib, E. Mottola and P. Tinyakov, *Winding transitions at finite energy and temperature: an $O(3)$ model*, *Phys. Rev.* **D 54** (1996) 7774 [hep-ph/9608327].

[24] K.L. Frost and L.G. Yaffe, *Periodic euclidean solutions of* SU(2)*-Higgs theory*, *Phys. Rev.* **D 59** (1999) 065013 [hep-ph/9807524];
*From instantons to sphalerons: time-dependent periodic solutions of* SU(2)*-Higgs theory*, *Phys. Rev.* **D 60** (1999) 105021 [hep-ph/9905224].

[25] G.F. Bonini, S. Habib, E. Mottola, C. Rebbi, R. Singleton and P. G. Tinyakov, *Periodic instantons in* SU(2) *Yang-Mills-Higgs theory*, hep-ph/9905243.

[26] D. Berenstein, R. Corrado, W. Fischler and J. Maldacena, *The operator product expansion for Wilson loops and surfaces in the large-$N$ limit*, *Phys. Rev.* **D 59** (1999) 105023 [hep-th/9809188].

[27] G. 't Hooft, *A planar diagram theory for strong interactions*, *Nucl. Phys.* **B 72** (1974) 461.

[28] E. Brezin, C. Itzykson, G. Parisi and J.B. Zuber, *Planar diagrams*, *Comm. Math. Phys.* **59** (1978) 35.

[29] A.A. Migdal, *Loop equations and 1/N expansion*, *Phys. Rep.* **102** (1983) 199.

[30] Y. Makeenko, *Loop equations in matrix models and in 2d quantum gravity*, *Mod. Phys. Lett.* **A 6** (1991) 1901.